THERMAL EFFECTS IN MULTICOMPONENT EQUIATOMIC Ni-BASED ALLOYS UNDER HIGH-ENERGY IRRADIATION WITH Kr IONS

I. V. Safronov,[1] V. V. Uglov,[1,2] A. O. Strechko,[1]
S. V. Zlotski,[1] J. Ke,[3] and G. E. Remnev[4]

Today, the concept of single-phase concentrated solid solutions offers an alternative strategy for increasing the radiation resistance of materials, namely, a multi-element composition with equiatomic or nearly equiatomic concentrations. It is highly desirable to understand the relationship between the chemical complexity of alloys and the thermal effects associated with irradiation in order to increase the radiation resistance of such materials. We present an analysis of the radiation heating, the thermoelastic stresses and the density of growth dislocations in the family of Ni-*based alloys:* NiCo–NiFe–NiCoFe–NiCoCr–NiCoFeCr–NiCoFeMnCr *exposed to high-energy irradiation with 145 MeV Kr ions performed by numerical modeling. The results show that the composition complexity of the alloys, especially that of* NiCoFeMnCr, *favors the radiation annealing of defects, decreases the level of hazardous thermoelastic stresses relative to the ultimate strength, and reduces the growth dislocation density compared to that in Ni.*

Keywords: radiation heating, thermoelastic stresses, dislocations, concentrated solid solutions, ion irradiation.

INTRODUCTION

Currently, single-phase alloys based on several principal elements or concentrated solid solutions attract an ever increasing attention due to a possibility of combining different properties, such as creep resistance, high-temperature strength, corrosion and radiation resistance, etc. [1]. In contrast to the traditional alloys, the elements in the concentrated solid solutions are found in equal (multi-component equiatomic alloys) or nearly equal atomic concentrations [2, 3].

In order to study the radiation damage of materials by the fission fragments, heavy ions with the energies from about 100 MeV to a few GeV are frequently used. In this case, the high rate and density of the released energy, which is nearly entirely transferred to the electron subsystem, causes a number of such effects as local melting, pressure wave generation, amorphization, etc. [4]. A molecular–dynamic simulation within the frames of a two -temperature model of the radiation response of the Ni and NiFe, NiCo alloys to an irradiation by a Bi ion with the energy of 1.542 GeV demonstrated an inhibition of the thermal energy dissipation in the alloys, which resulted in the formation of a molten cylindrical region along the ion path in them; this however was not observed in Ni [5]. A concurrent experiment involving processing of the scanning electron microscopy data from the irradiated Ni- and NiFe-samples (1.542 GeV Bi^{+}, $2 \cdot 10^{12}$ cm^{-2}, 300 K) demonstrated a higher level of the radiation damage (interstitial dislocation loops and stacking fault tetrahedra) in the NiFe alloy [5]. However, in the case of irradiation of Ni-containing alloys by Ni ions with the

[1]Belarusian State University, Minsk, Republic of Belarus e-mail: fiz.safronov@mail.ru; uglov@bsu.by; grontgront@gmail.com; zlotski@bsu.by; [2]National Research Nuclear University MEPhI, Moscow, Russia; [3]Beijing Institute of Technology, Beijing, China, e-mail: hbli@mail.ipc.ac.cn; [4]National Research Tomsk Polytechnic University, Tomsk, Russia, e-mail: remnev@tpu.ru.

energy of 1.5 MeV ($1 \cdot 10^{14}$ cm^{-2}, 300 K) the results demonstrated a decrease of the radiation damage in the sequence from Ni, NiCo, NiFe/NiCoFe to NiCoFeCr/NiCoCr, which correlates with the decrease in their heat conduction [6]. Earlier an idea was put forward that one of the factors inhibiting the defect accumulation in the concentrated solid solutions under the conditions of their room-temperature irradiation is low heat conduction [7]. This gives rise to slower thermal energy dissipation and, hence, longer thermal peak stages and the radiation defect recombination [8]. Nevertheless, it is clear from the two above-cited experimental results that the effect of heat conduction does not prevail in simple cases (Ni, NiFe). A study of the defect evolution in Ni-containing alloys (Ni, NiCo, NiFe, NiCoFe, NiCoCr) during the low-energy molecular-dynamics simulation of the collision cascades (5 keV, 300 K) demonstrated that a sophistication of the alloy compositions, on the whole, reduces the susceptibility to defect accumulation; however in simple cases (Ni, NiCo) this is not observed [9]. The authors also demonstrated a correlation between the radiation damage level and the dislocation mobility. They found out that both the least level of the accumulated defects and the lowest dislocation mobility are typical for the NiCoCr alloy [9].

Considering that the earlier theoretical studies were limited to the discussion of some of the Ni-containing equiatomic alloys (binary, ternary) and modeling of their radiation response under the low-energy impact, it is appealing to study such an aspect as thermal effects during irradiation with high-energy ions (Kr) in the family of Ni-based alloys (NiCo–NiFe–NiCoFe–NiCoCr–NiCoFeCr–NiCoFeMnCr) in order to estimate the influence of their elemental composition. To this end, we analyzed the radiation heating, thermoelastic stresses and growth dislocation density. The calculations are limited to a single-temperature model with constant coefficients.

MODELING PROCEDURE

The theoretical objects were the following Ni-based equiatomic alloys: NiCo–NiFe–NiCoFe–NiCoCr–NiCoFeCr–NiCoFeMnCr subjected to irradiation with high-energy Kr ions. The irradiation parameters were: bombarding ion energy – 145 MeV, fluence – $1 \cdot 10^{14}$ cm^{-2}, irradiation temperature – 300 K. The research focused on the radiation (high-temperature) heating, the thermoelastic stresses and the density of growth dislocations generated under certain conditions of the radiation heating.

There are a number of approaches to calculating the temperature in the vicinity of the ion track, which, among other things, include the interaction between the electron and ion subsystems of a material [4]. The approach relying on a two-temperature model with variable coefficients and taking into account the phase transformations [4] is quite efficient. However, there is a limiting factor to its application: the absence of such initial data as the dependence of the coefficients of the lattice and electron thermal conductivity on the temperature in a wide range of values and the latent melting and vaporization heat values.

In this study, instead of the term ‘track’ we are going to use the term ‘a region around the ion trajectory’, due to the fact that the alloys under consideration exhibit a metallic bonding, and there is no answer to what is the threshold loss of the electron energy, above which the track formation is observed [4]. Approximating the region around the ion trajectory with a cylinder, in order to estimate the temperature beyond this region (in the external region), let us use an expression from our earlier work [10]

$$T(r,t) \; T_0 \; \frac{dE/dz}{4} \frac{e^{-\frac{r^2}{4t}}}{t}, \qquad (1)$$

where T_0 is the initial target temperature, dE/dz is the specific ion energy loss, λ is the heat diffusion coefficient (thermal diffusivity), κ is the heat conduction coefficient (thermal conductivity), r is the radial coordinate, z is the depth coordinate, t is the time.

Expression (1) is the solution to a classical heat conduction equation of a parabolic type with an instantaneous heat source and a constant coefficient within the frames of a one-temperature model. After the test calculations in the SRIM/TRIM program, including considerable ionization loss (~97%), the average value of the electron energy loss

dE_{el}/dz was taken to be dE/dz over the entire depth H for every target $\frac{1}{H}\int_0^H \frac{dE}{dz}^{*} dz$. In their turn, the data for the thermal diffusivity and conductivity were taken from [11].

Thermoelastic stresses were estimated using the following formula [12]:

$$T(r,t) \quad B\,T(r,t) \quad T_0 \ , \tag{2}$$

where α is the coefficient of linear thermal expansion (CLTE), B is the bulk modulus. The values of the CLTE and bulk modulus were taken from [11] and [13], respectively.

The dislocations were generated under certain conditions of the radiation heating. The dislocation density was estimated by the following formula [12]:

$$n_d(r,t) \quad \frac{1}{b} \left| T \quad {}_r \right| T \quad {}_{cr} \ , \tag{3}$$

where b is the absolute value of the Burgers vector (~ lattice parameter a_0), $|T_r|$ is the absolute value of the radial temperature gradient, $T_{cr} \quad Gl^{cr}$, $_{cr}$ is the critical stress, G is the shear modulus, l is the size of the zone where $T_r \; T$ $_{cr}$. The lattice parameter and shear modulus data were taken from [11] and [13], respectively.

RESULTS AND DISCUSSION

Figure 1 presents the distribution profile of the specific energy loss of Kr ions over the depth during their deceleration in pure Ni and in the NiCoFeMnCr alloy. The distribution profiles for other alloys lie between Curves *1* and *2* for the electron energy loss (dE_{el}/dz) and between Curves *2* and *4* for the nuclear energy loss (dE_{nuc}/dz) (Fig. 1). The difference here is due to the compositional effect determining a complex influence of the charge number, atomic mass of the target, etc. on the deceleration of ions. According to the SRIM simulation results (Fig. 1), the lowest electron energy loss is observed in the NiCoFeMnCr alloy and the highest loss – in Ni at the depths of approximately 5 μm. Numerically, the difference between the minimum and maximum values for all of the alloys in question is a few units of keV/nm. The maximum electron energy loss exceeds the nuclear energy loss by more than a factor of 800. A substantial electron energy loss (of more than 5 keV/nm) at the depths to about 8 μm is included into the prediction of radiation heating of the zones followed by their melting or boiling. The zones of the highest radiation damage associated with the atomic displacements (disordering) in the target are found at the depths of ~ 8−9 μm, depending on the alloy composition.

The data on the averaged electron energy loss were used to calculate the temperature in the external region around the ion trajectory via formula (1). According to the theory, the stages of thermal peaks, recombination and annealing start ~10^{-12} s after the stage of a collision cascade development of ~10^{-14}–10^{-13} s. Therefore, in this work the time counting starts from the 1st picosecond, taking that from this time the atomic velocity distribution is approximately described by the Maxwell distribution, and one can introduce a local temperature notion.

Figure 2 presents the temperature profiles in the external region around the ion trajectory in the alloys under study at the initial time point (1 ps). According to the calculation results, the highest temperatures at the initial time are achieved in the alloys containing Ni, Co and Cr – NiCoCr, NiCoFeCr and NiCoFeMnCr, while the lowest temperatures – in Ni and NiCo. This is due to the effect of both the electron energy loss (Fig. 1) and the thermal conductivity and diffusivity (Table 1) on the value of the temperature. It follows from expression (1) that a reduction of the electron energy loss, an increase of the thermal conductivity and a decrease of the thermal diffusivity would result in a lower radiation heating of the target. A higher radiation heating of the NiCoCr-, NiCoFeCr- and NiCoFeMnCr alloys is primarily conditioned by their low thermal conductivity (Table 1). It is clear from Fig. 2 and the data of Table 1 that the

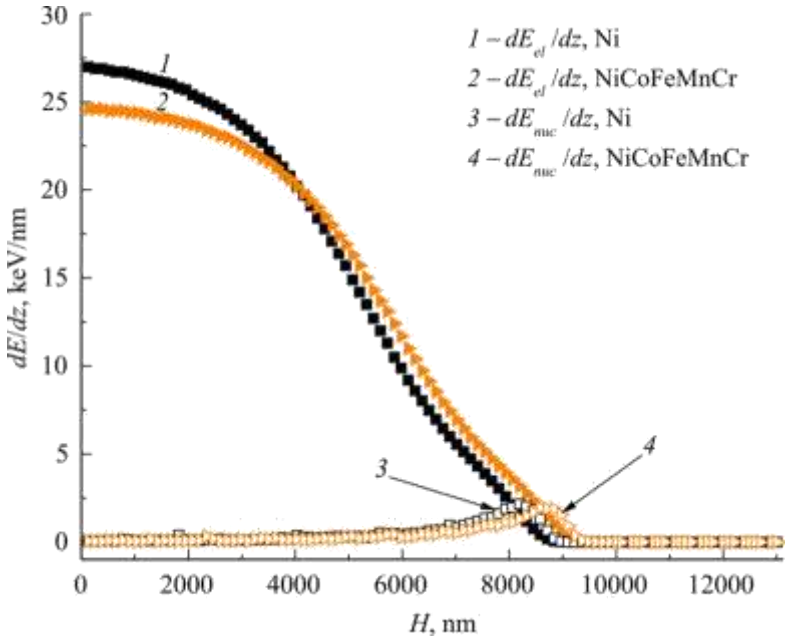

Fig. 1. Specific energy loss of Kr ions (145 MeV) in Ni and NiCoFeMnCr alloy. The notation legend: dE_{el}/dz – electron energy losses, dE_{nuc}/dz – nuclear energy losses.

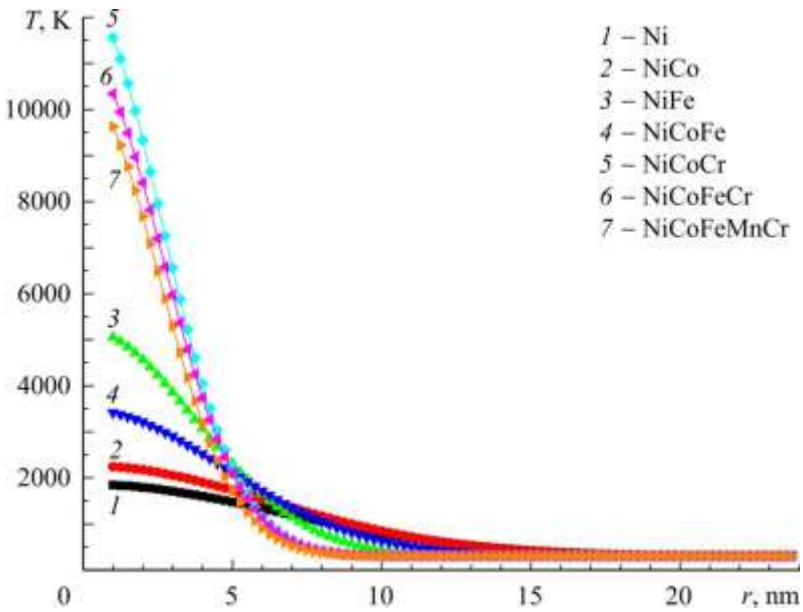

Fig. 2. Temperature profiles in the external region around the Kr ion trajectory (145 MeV) in the alloys at the initial time of 1 ps.

temperatures in the neighborhood of the ion trajectory exceed the alloy melting temperatures T_m. An estimation of the radiation heating in the binary NiCo - and NiFe alloys is qualitatively consistent with the results of the molecular-dynamic simulation within the frames of a two-temperature model (hybrid method) [5].

TABLE 1. Thermophysical Data of Ni-based Alloys

Alloys	T_m [13], K	κ (300 K) [11], W/(m·K)	λ (300 K) [11], 10^{-6} m^2/s
Ni	1728	88.0	22.0
NiCo	1735	69.9	19.5
NiFe	1703	28.0	6.95
NiCoFe	1724	43.3	11.1
NiCoCr	1690	11.4	3.40
NiCoFeCr	1695	12.8	3.50
NiCoFeMnCr	1553	13.7	3.20

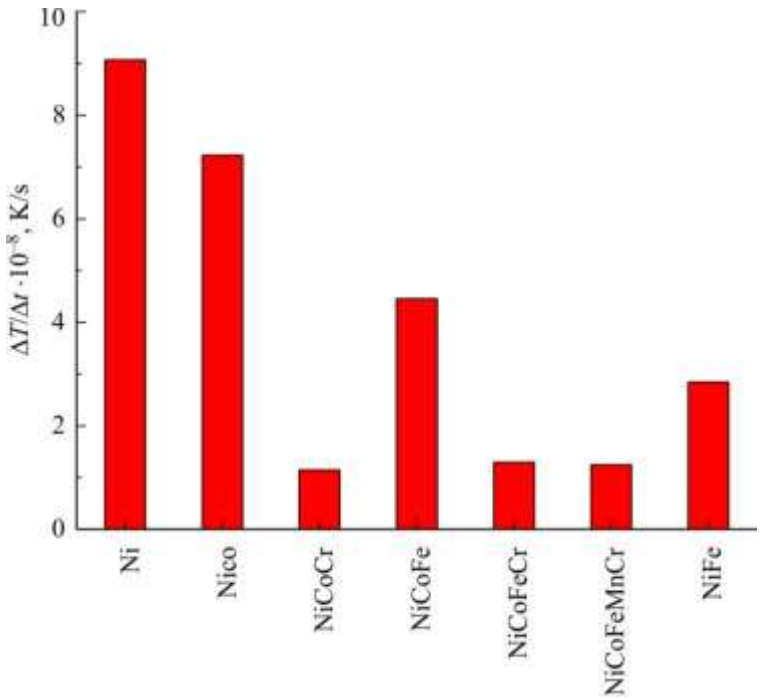

Fig. 3. Diagram of the average maximum cooling rate of the alloys.

Not least important is the issue of estimating the alloy cooling rate. We examined the average maximum alloy cooling rate, which was calculated using the incremental ratio $\Delta T/\Delta t$, where the initial temperature was the alloy melting temperature at the respective time point (when any given alloy is cooled to its T_m). The final temperature was room temperature (300 K) and, hence, the time when the alloy reaches this T with an error of 0.001 K. The cooling rate is the highest because T is calculated in the vicinity of the area around the ion trajectory. Figure 3 presents the diagram of the average maximum alloy cooling rate. It is seen in Fig. 3 that the lowest cooling rates characterize the NiCoCr-, NiCoFeCr- and NiCoFeMnCr alloys, which is consistent with their low thermal conductivity values. It is known that high cooling rates can give rise to amorphization of the cascade damage regions. Relying on the results obtained, we can make a conclusion concerning the most effective defect structure annealing in the NiCoCr-, NiCoFeCr- and NiCoFeMnCr alloys. According to the introduction to this article, a reduced thermal conductivity results in a slower thermal energy dissipation and, thus, in longer thermal peak stages and defect recombination [8], due to which there is a correlation between the thermal conductivity and the level of radiation damage in the equiatomic alloys under consideration in the case of their irradiation at room temperature to low fluences [6].

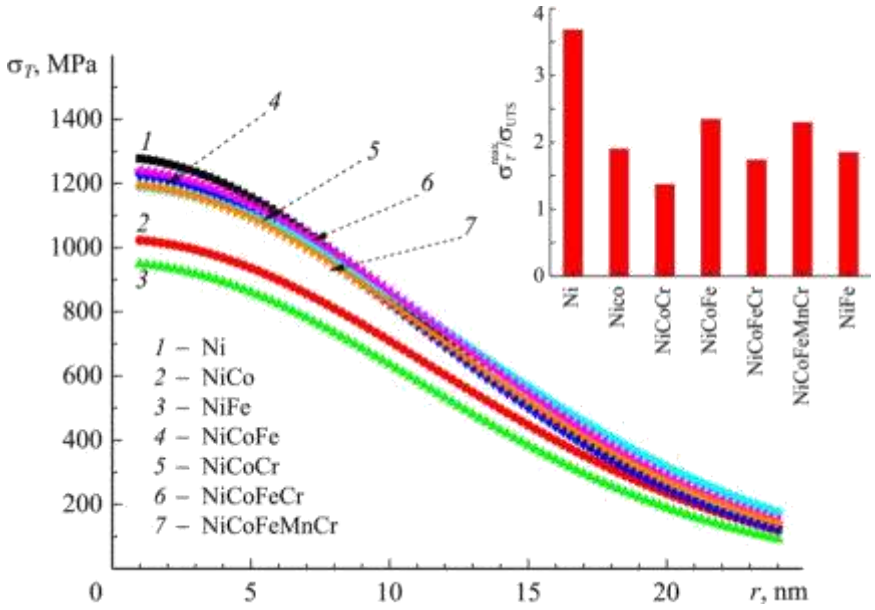

Fig. 4. Spatial distribution of thermoelastic stresses in the external region around the ion trajectory in the alloys after cooling of the molten zones to below $0.5T_m$. The insert shows the ratio of the maximum thermoelastic stresses $T^{\max}$ to the ultimate tensile strength σ_{UTS} of the alloys.

Due to the high temperatures, thermal stresses would develop around the ion trajectory. Here we analyze the elastic part of the stresses only. Figure 4 presents the thermoelastic stresses in the alloys after cooling of the molten zones to below $0.5T_m$.

According to the calculations, the highest thermoelastic stress values are typical for Ni, and the lowest – for the NiFe alloy. In the NiCoCr-, NiCoFeCr- and NiFeCoMnCr alloys, the thermoelastic stresses are 40−90 MPa lower than in Ni. These relationships are determined by the respective contribution of two multipliers (see expression (2)), one of which characterizes the thermomechanical alloy properties in the form of a product of the CLTE and the bulk modulus, and the other – the radiation heating via T. However, given the fact that here we discuss the elastic part of thermal stresses only, it is reasonable to take a certain part of T_m, e.g., $0.5T_m$, as an upper temperature bound. Figure 5 presents the enumerated characteristics. The difference in their values determines the curves of dependence given in Fig. 4.

Based on the plots given in Fig. 4, we revealed that the most hazardous level of thermoelastic stresses $T^{\max}$ compared to the ultimate tensile strength σ_{UTS} is found in pure Ni. Their ratio is minimal for the NiCoCr alloy (Fig. 4). The σ_{UTS} (300 K) data for the alloys were taken from [13].

The thermal stresses, being dynamic stresses, decline very rapidly as the alloys undergo cooling. The role of these stresses consists in an additional influence on the evolution of the alloy microstructure. Given a lower cooling rate of the NiCoCr-, NiCoFeCr- and NiFeCoMnCr alloys (Fig. 3), the thermoelastic stresses in the latter would operate for a longer period of time than in the other alloys and Ni. Considering that a more sophisticated composition inhibits the sluggish diffusion effect [6], this would reduce the defect migration ability under the action of different forces formed in different stages of the collision cascade evolution [14]. Therefore, it is expected that in the NiCoCr-, NiCoFeCr- and NiFeCoMnCr alloys the non-diffusion defect migrations under the action of, e.g. thermoelastic stresses, would be less substantial than in Ni. For instance, a considerably higher suppression of the radiation-induced segregation was found out [15] in the NiCoFeCr- and especially in NiFeCoMnCr alloys compared to the NiFe- and NiCoFe alloys, which the authors attribute to the sluggish diffusion effect. It should be added that the maximum sluggish diffusion effect is observed near the percolation threshold for the alloy component concentration [16]. For the face-centered cubic lattice,

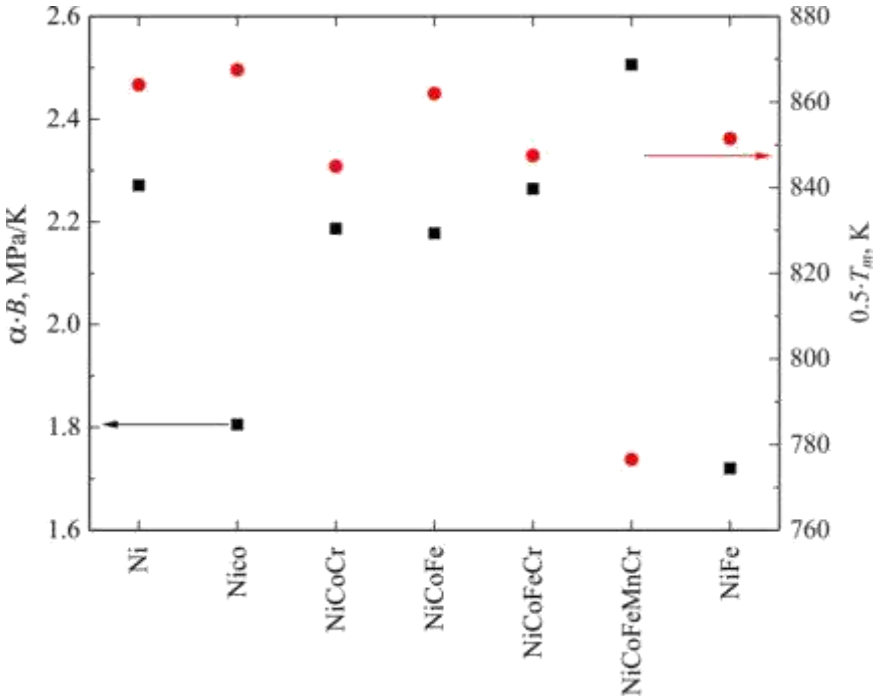

Fig. 5. Contribution of multipliers in expression (2) for determination of the maximum values of thermoelastic stresses.

the value of this characteristic is equal to 0.25 (1/5), where 5 is the number of components for which there is no percolation over the sites (of continuous binding) for each element.

As far as the residual stresses are concerned, they are known to be related to the defect structure, and in their value these stresses are substantially lower than the radiation-induces stress. However, omitting the study of the defect evolution, it is quite difficult to relate the level of dynamic stresses to the subsequent residual stresses. Nevertheless, the experimental data [17] demonstrate that the total elastic deformation in NiCoFeCr after irradiation with Ni ions is larger than that in NiFe, which is due to the presence of smaller defect clusters and hence their higher density.

Radiation heating can also cause a generation of growth dislocations due to the temperature gradient at the crystallization front. Figure 6 gives the dislocation density distribution in the external region around the ion trajectory in the alloys after cooling of the molten zones to lower than $0.2T_m$. It is seen from the distribution curves that the highest dislocation densities are achieved in Ni, and the lowest – in the NiCoFeMnCr alloy. Analyzing expression (3), we realize that the dislocation density value is determined by a contribution of two multipliers: the alloy characteristics in the form of a ratio of the CLTE to the absolute value of the Burgers vector and the radial temperature gradient. A combined contribution of these multipliers, demonstrated in Fig. 7, determines the curves of dependence given in Fig. 6. It is worthy of mention that expression (3) describes only the generation of growth dislocations during the radiation heating and does not include their further evolution (redistribution, interaction, accumulation), therefore the dislocation densities cannot be compared with a certain final value, which would be characteristic for the assigned radiation parameters. This is due to the fact that the formation of dislocation structure is a complex process, starting from a combination of point defects in close- packed planes and further involving the formation, growth and transformation of dislocation loops, whose further growth and crossing results in the formation of a certain dislocation network. The generation of growth dislocations is thought to be an additional mechanism.

The results of earlier investigations [15] demonstrate that a sophistication of the alloy compositions gives rise to an increase in the concentration of the defective (imperfect) interstitial-type dislocation loops. The latter indicates an extension of the incubation period and an inhibition of the loop growth [15]. According to the experimental data [15], the dislocation loop concentration in certain alloys increases in the following sequence: NiFe < NiCoFeCr < NiCoFe <

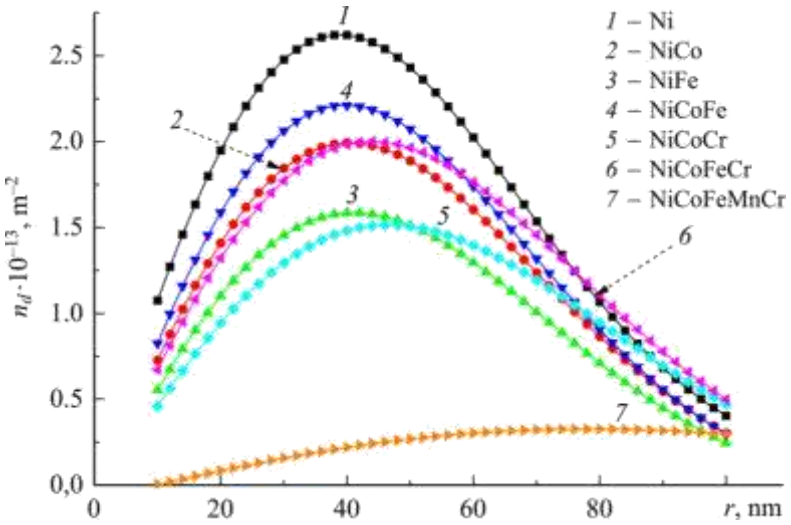

Fig. 6. Distribution of the growth dislocation density in the external region around the ion trajectory in the alloys after cooling of the molten zones to below $0.2T_m$.

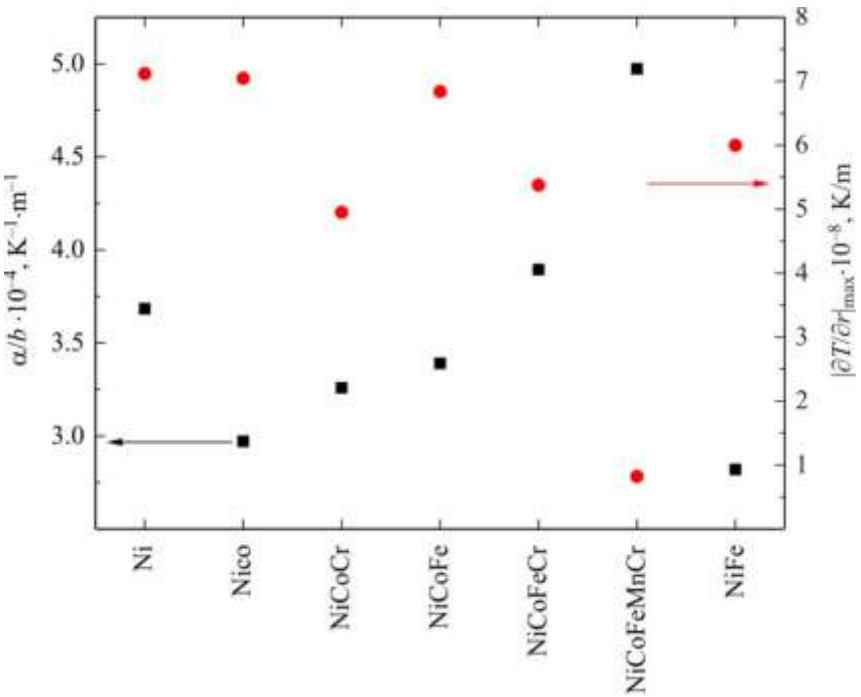

Fig. 7. Contribution of multipliers in expression (2) for determination of the maximum values of dislocation density.

NiCoFeMnCr (the case of irradiation with high-temperature Ni ions to a high fluence). It is known that for the pores to nucleate under irradiation of the material it is necessary to achieve a so- called critical dislocation density; e.g., in Ni its value is about 10^{13} m^{-2} [18]. In accordance with the experimental data, the radiation swelling stability increases in the following sequence: Ni < NiCo < NiCoCr < NiFe ≤ NiCoFeCr < NiCoFe ≤ NiCoFeMnCr (the case of irradiation with high-temperature Ni ions to a high fluence) [19]. Therefore, based on the results obtained we can draw a conclusion that

there is a tendency towards a decrease in the density of growth dislocations due to the sophistication of the alloy composition.

To sum up, a more sophisticated alloy composition, especially such as NiCoFeMnCr, favors the defect annealing, decreases the level of hazardous thermoelastic stresses compared to the ultimate tensile strength, and decreases the density of growth dislocations compared to Ni.

CONCLUSIONS

In this work, an analysis has been performed of such thermal effects as radiation heating, thermoelastic stresses and generation of growth dislocations in the family of Ni-based equiatomic alloys: NiCo–NiFe–NiCoFe–NiCoCr–NiCoFeCr–NiCoFeMnCr after their irradiation with high-energy Kr ions with the energy of 145 MeV. The calculations of the temperature fields and the related thermoelastic stresses and the dislocation density were performed using the analytical expressions. The specific ion energy losses were simulated in the SRIM/TRIM software program in a mode of the detailed damage cascade calculation.

The research results have demonstrated that the most efficient defect structure annealing is more characteristic for NiCoCr- , NiCoFeCr- and NiCoFeMnCr alloys compared to other Ni-based alloys. This was demonstrated based on the analysis of the average alloy cooling rate, which is consistent with the conclusions of other authors concerning the correlation between the thermal conductivity and the level of radiation damage. Proceeding from the calculation of thermoelastic stresses, we have found that the most hazardous level of thermoelastic stresses compared to the ultimate tensile strength is observed in pure Ni. One must bear in mind that a sophistication of the alloy composition results in a decrease of the $T^{\max} / \sigma_{\mathrm{UTS}}$ ratio, and the minimal value is characteristic for the NiCoCr alloy. Furthermore, a tendency has been noted in this study that a more sophisticated alloy composition gives rise to a lower density of growth dislocations due to the presence of a temperature gradient.

The results obtained in this investigation reveal a correlation between the chemical complexity of equiatomic alloys and their thermophysical characteristics in terms of improving their radiation stability, especially for the NiCoFeMnCr alloy.

There are certain disadvantages in this study. The character of the thermophysical relationships is mainly controlled by the values of thermal conductivity and electron energy losses, affecting the radiation heating of the target, and by the values of the static contributions from the coefficients entering the formulas for calculating the thermoelastic stresses and dislocation density, which is an idealization. For estimating the radiation heating, we used a solution to the heat equation of a parabolic type with the constant coefficients for a one-temperature model, which is a rather rough approximation. An inclusion into consideration of temperature relations, phase transitions, electron subsystem temperature and electron-phonon interaction, as well as of an additional term describing the final heat propagation velocity would open up new prospects for future research. It is evident that currently it is possible to find a solution to a generalized heat conduction (hyperbolic) equation only numerically. Given the correct interatomic interaction potentials, it appears that the method of a two-temperature molecular dynamics would be more exact and successful.

This study was partially supported by a grant from BRFFR, Project No. T20BIT-009 (BITBLR2020019). The numerical modeling was performed using the software programs of a high-performance cluster of NR TPU.

REFERENCES

1. D. B. Miracle and O. N. Senkov, Acta Mater., **122**, 448 (2017).
2. J. W. Yeh, S. K. Chen, S. J. Lin, *et al*., Adv. Eng. Mater., **6**, 299 (2004).
3. B. Cantor, I. T. H. Chang, P. Knight, *et al*., Mater. Sci. Eng. A, **375**, 213 (2004).
4. F. F. Komarov, UFN, **173**, No. 12, 1287 (2003).
5. A. A. Leino, G. D. Samolyuk, R. Sachan, *et al*., Acta Mater., **151**, 191 (2018).
6. K. Jin and H. Bei, Front. Mater., **5**, No. 26, 1 (2018).
7. Y. Zhang, G. M. Stocks, K. Jin, *et al*., Nat. Commun., **6**, No. 8736, 1 (2015).

8. M. W. Ullah, D. S. Aidhy, Y. Zhang, *et al*., Acta Mater., **109**, 17 (2016).
9. E. Levo, F. Granberg, C. Fridlund, *et al*., J. Nucl. Mater., **490**, 323 (2017).
10. V. V. Uglov, N. T. Kvasov, N. D. Komarov, *et al*., Russ. Phys. J., **62**, No. 4, 115 (2019).
11. K. Jin, S. Mu, K. An, *et al*., Mater. Des., **117**, 185 (2017).
12. V. V. Uglov, N. T. Kvasov, V. I. Shimanskii, et al., Russ. Phys. J., **60**, No. 10, 125 (2017).
13. Z. Wu, H. Bei, G. M. Pharr, *et al*., Acta Mater., **81**, 428 (2014).
14. V. V. Uglov, G. E. Remnev, N. T. Kvasov, *et al*., J. Synch. Investig., **8**, 703 (2014).
15. C. Lu, T. Yang, K. Jin, *et al*., Acta Mater., **127**, 98 (2017).
16. Y. N. Osetsky, L. K. Beland, A. V. Barashev, *et al*., Curr. Opin. Solid State Mater. Sci., **22**, Iss. 3, 65 (2018).
17. Y. Zhang and W. J. Weber, Appl. Phys. Rev., **7**, 041307-1-35 (2020).
18. J. E. Harbottle, Philos. Mag.: J. Theor. Exp. Appl. Phys., **27**, Iss. 1, 147 (1973).
19. K. Jin, C. Lu, L. M. Wang, *et al*., Scripta Mater., **119**, 65 (2016).